minerals

MDPI

Article

Synchrotron Nano-Diffraction Study of Thermally Treated Asbestos Tremolite from Val d'Ala, Turin (Italy)

Carlotta Giacobbe [1,*], Jonathan P. Wright [1], Dario Di Giuseppe [2], Alessandro Zoboli [2], Mauro Zapparoli [3] and Alessandro F. Gualtieri [2]

[1] European Synchrotron Radiation Facility, 71 Avenue des Martyrs, 38040 Grenoble, France; wright@esrf.fr
[2] Department of Chemical and Geological Sciences, University of Modena and Reggio Emilia, I-41121 Modena, Italy; dario.digiuseppe@unimore.it (D.D.G.); 176695@studenti.unimore.it (A.Z.); alessandro.gualtieri@unimore.it (A.F.G.)
[3] CIGS, University of Modena and Reggio Emilia, I-41121 Modena, Italy; mauro.zapparoli@unimore.it
* Correspondence: carlotta.giacobbe@esrf.fr; Tel.: +33-(0)476881754

Received: 29 June 2018; Accepted: 20 July 2018; Published: 24 July 2018

Abstract: Nowadays, due to the adverse health effects associated with exposure to asbestos, its removal and thermal inertization has become one of the most promising ways for reducing waste risk management. Despite all the advances in structure analysis of fibers and characterization, some problems still remain that are very hard to solve. One challenge is the structure analysis of natural micro- and nano-crystalline samples, which do not form crystals large enough for single-crystal X-ray diffraction (SC-XRD), and their analysis is often hampered by reflection overlap and the coexistence of multiple fibres linked together. In this paper, we have used nano-focused synchrotron X-rays to refine the crystal structure of a micrometric tremolite fibres from Val d'Ala, Turin (Italy) after various heat treatment. The structure of the original fibre and after heating to 800 °C show minor differences, while the fibre that was heated at 1000 °C is recrystallized into pyroxene phases and cristobalite.

Keywords: asbestos; tremolite; synchrotron radiation; nano-diffraction; recrystallization

1. Introduction

Asbestos is a commercial term which includes six minerals: Chrysotile (serpentine asbestos) and five fibrous amphiboles (actinolite asbestos, amosite, anthophyllite asbestos, crocidolite, and tremolite asbestos) [1,2].

The outstanding chemical-physical and technological properties of asbestos minerals are well known since about 5000 years ago [3] and more than 3000 industrial applications of asbestos containing materials (ACMs) are known to date [4]. Unfortunately, although with different intensity, these minerals are also known for their toxicity/pathogenicity potential and they can cause lung diseases if inhaled. For this reason, they are classified as carcinogenic substances *Group*1 by the International Agency for Research on Cancer (IARC) [5] and many countries have banned their use [4]. Today, most European countries have a policy to safely remove and dispose ACMs. In these countries where remediation policies are encouraged, many studies and patents have dealt with the possible disposal via thermal inertization and recycling of ACMs (see a selection in refs. [6–12]).

In parallel to the studies on the applications of the thermal treatment and recycling of ACMs, more basic studies on the high temperature transformation of asbestos minerals at a molecular scale are being conducted, although they mostly focussed on the commercial asbestos forms chrysotile, crocidolite, and amosite (see ref. [13] for example).

Asbestos tremolite is often associated with chrysotile in natural occurrences. Deepening the knowledge of its thermal behaviour is of utmost importance, as it can be one of the hazardous phases to destroy during the thermally induced inertization of ACMs. Tremolite is a monoclinic ($C2/m$) calcic amphibole with ideal formula $Ca_2Mg_5Si_8O_{22}(OH)_2$. The tremolite amphibole structure consists of two principal elements, a double chain of corner sharing tetrahedra and a strip of edge-sharing octahedra, both of which extend in the **c**-direction [14]. The tetrahedrally coordinated sites are denoted by *T* and ideally occupied by Si, while the octahedrally coordinated sites are denoted by *M*. There are three distinct types of octahedra that are designated *M*(1), *M*(2), and *M*(3), occupied by Mg in tremolite. At the junction of the strip of octahedra and the chain of tetrahedra is the *M*(4) site ideally occupied by Ca in tremolite, and below the hexagonal ring of tetrahedra is the A site at the centre of a large cavity which is empty in tremolite [14–16]. The study of the thermal behaviour of tremolite started more than 60 years ago (see the review in [17]). The early work by Wittels [18] showed that water was released at about 1125 °C following the reaction: $Ca_2Mg_5Si_8O_{22}(OH)_2 \rightarrow 2CaSiO_3 + 5MgSiO_3 + SiO_2 + H_2O$. After heating, tremolite forms pyroxenes, silica, and water, revealing a mechanism of structural collapse whereby the double-chain units split into single-chain units. Kusiorowski et al. [19] showed that its thermal decomposition started at 950 °C and Bloise et al. [20] showed that the breakdown of tremolite asbestos from Val d'Ala (Italy) occurred at 1046 °C. The following reaction path during the thermal decomposition of tremolite has been postulated [21]: (1) The atomic bonds undergo thermal expansion and the A sites expand [22]; (2) two adjacent hydroxyls on the *M*(1) sites condensate to water via $2OH^- \rightarrow H_2O + O_2^-$; (3) water diffuses outside the crystal lattice; (4) the remaining cation atoms reorganize by a reconstructive mechanism; (5) Si-rich *T* sites shift to maintain electronic neutrality. As anticipated, the final mineral assemblage after the decomposition of the tremolite above 1100 °C is composed of diopside ($CaMgSi_2O_6$), enstatite ($MgSiO_3$), and cristobalite. EDS spot analyses confirmed that the pseudomorphic process involved a complete recrystallisation of the original tremolite asbestos into diopside [20].

In this work, a novel nano-diffraction study was performed on asbestos tremolite and its high temperature reaction products at 800 and 1000 °C. The nano-diffraction experiments were conducted at beamline ID11 at the European Synchrotron Radiation Facility (ESRF) in Grenoble (France).

2. Materials and Methods

A tremolite asbestos sample from the serpentinites of the Ultrabasic Lanzo Massif in the Occidental Alps (Lanzo Valley, Piedmont) was selected for the study. A detailed characterization of this mineral fibre is reported in [23]. Its chemical formula is: $(Ca_{1.91}Na_{0.06}K_{0.01})_{1.98}(Mg_{4.71}Fe^{2+}_{0.22}Fe^{3+}_{0.08}Mn_{0.02})_{5.03}(Si_{8.01}Al_{0.02})_{8.03}O_{22.14}(OH)_{1.86}$.

The sample contains minor impurities of antigorite and clinochlore, its mean fibre length is 11(1) μm, and the specific surface is 9.2(3) m^2/g. The raw sample was heated in a high temperature furnace at 800 °C and 1000 °C for 30 min and quenched in air to obtain the high temperature products of transformation.

Single crystal nano-diffraction data sets of the RT (room temperature), 800 °C and 1000 °C treated tremolite fibres have been collected at the beamline ID11 (ESRF, The European Synchrotron Radiation Facility, Grenoble, France), using a monochromatic beam produced by a bent Si (111) Laue–Laue double-crystal monochromator (40 keV, wavelength $\lambda = 0.309$ Å, relative bandwidth $\Delta\lambda/\lambda \approx 10^{-3}$). The beam was focused to 500 nm in horizontal direction and 300 nm in vertical direction with a Si refractive compound lenses system [24]. On the "nanoscope" station, the sample centring and scanning are operated via a *NanoPos* hexapod (Symétrie) mounted on a piezoelectric xyz stage. The minimum incremental movement is 10 nm in the vertical and in the two horizontal directions. The single-crystal fibres (ca. 40 μm × 3 μm) were centred in the beam with the help of the standard deviation signal recorded by the diffraction camera. The diffracted signals have been collected by a 2D detector (Frelon Camera [25]) placed at 112.3 mm from the sample. The sample-to-detector-distance and detector tilt have been calibrated using a sucrose single crystal. A series of images (typically 1800) have been

recorded while the sample was rotating through 360° (with a resulting step-size per image of 0.2°) with an exposure time of 1 s. Images were then converted into the "Esperanto" format using an in-house software (FREAC) script in order to be processed with the Crysalis software [26]. Bragg peaks were indexed and their intensities were integrated and corrected for Lorentz polarization effects, using the *CrysAlis* package. Scaling and correction for absorption was applied by the semi-empirical ABSPACK routine implemented in CrysAlis. For the structure refinements, synchrotron datasets were used up to a resolution of 0.55 Å (R_{int} = 0.025). The final list of reflections with the indices and intensities was output to an HKL file in a standard HKL format. After data integration structures were solved and refined by direct methods and refined on F^2 with the SHELX program suite [27].

High Resolution powder diffraction data have been acquired at the ID22 beamline (ESRF) for the tremolite sample treated at 1000 °C. The powder has been gently ground with an agate mortar and pestle, introduced into 0.5 mm diameter borosilicate glass capillaries and spun at 787 rpm to minimize preferred orientation effect. The powder diffraction pattern has been collected at 25 keV (λ = 0.49600 Å, calibrated with the Si NIST standard SRM 640c at room temperature), with a beam size of 1 mm (horizontal) by 0.9 mm (vertical) defined by water-cooled slits and monochromated with a cryogenically cooled Si 111 channel-cut crystal. A bank of nine detectors, each preceded by a Si 111 analyser crystal, was scanned vertically to measure the diffracted intensity. The full profile fitting analyses were performed using XRPD data and Rietveld refinements. The Rietveld refinement has been performed using the GSAS [28] package and its graphical interface EXPGUI [29].

Field emission gun-Scanning electron microscopy (FEG-SEM) on the fibres heated at 800 and 1000 °C performed using a FEI Quanta Nova NanoSEM 450 (Milano, Italy) instrument.

3. Results

3.1. X-ray Single Crystal Nano-Diffraction

Table 1 shows the result of the first single crystal nano-diffraction experiment performed on an asbestos fibre. The nanodiffraction experiment allowed us to refine the crystal structure of the raw tremolite at RT and 800 °C. The data at 1000 °C shows recrystallization of the fibre and a multiphase assemblage (see below). Table 2 reports the possible population scheme for the tremolite at RT, as derived from the unit formula obtained by chemical analysis, including Mössbauer [30] and the result of the structure refinement (present results). Table 3 reports the structural data of RT and 800 °C asbestos tremolite as obtained from the refinement using the single crystal nano-diffraction data. Atomic positions, occupancies and atomic displacement parameters (a.d.p.) are respectively reported.

Table 1. Unit cell parameters and crystallographic details for the room temperature (RT) and 800 °C tremolite fibres.

	RT	**800 °C**
a (Å)	9.8536(2)	9.9044(2)
b (Å)	18.0774(3)	18.1311(2)
c (Å)	5.2843(1)	5.3009(3)
β (°)	104.709(2)	104.687(2)
V (Å^3)	910.44	917.1
Space group	*C*2/*m*	*C*2/*m*
Size (μm)	4.3	5.8
GooF	1.021	1.022
R_1	4.07	4.99
wR2	0.1175	0.118

Table 2. Population scheme of the raw tremolite sample as it results from the combination chemical, including Mössbauer [30] and refinement data.

Tremolite RT	Refinement	Possible Site Partition	Chemical Data
M(4)	40.00		
B site sum	40.00	$Ca_{1.91}Na_{0.06}K_{0.01}$	39.05
M(1)	25.23	$Mg_{1.884}Fe^{2+}{}_{0.088}Mn_{0.02}$	25.40
M(2)	26.30	$Mg_{1.884}Fe^{2+}{}_{0.088}Fe^{3+}{}_{0.08}$	26.98
M(3)	12.62	$Mg_{0.942}Fe^{2+}{}_{0.044}$	12.44
C sites sum	64.15		64.82

3.2. X-ray Powder Nano-Diffraction

The data collection at 1000 °C revealed that the fibre has undergone recrystallization. Figure 1 reports an example of 2D diffraction image collected on the tremolite fibre heated at 1000 °C with the *d*-spacings in Å of the major diffraction lines. The observed crystalline phases are diopside (di), enstatite (en), and clinoenstatite (cen). Figure 2 is the graphical result of the Rietveld refinement of the bulk fibrous tremolite sample heated at 1000 °C. The agreement factors of the refinement are: R_p = 8.51%, R_{wp} = 5.90%, and χ^2 = 12.35. The obtained quantitative phase analysis (wt %) is: Diopside 89.7(3), cristobalite 7.3(4), clinoenstatite 2.1(4), protoenstatite 0.7(3), and calcite (secondary) 0.2(1).

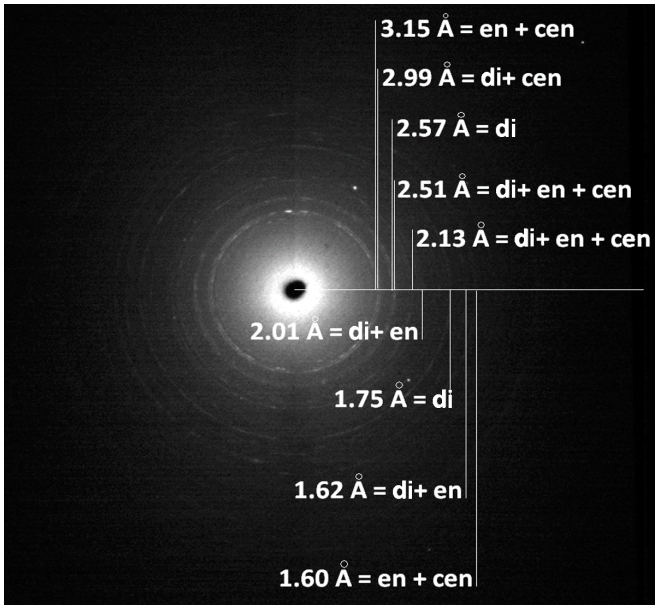

Figure 1. Interpretation of the nanodiffraction image collected on a tremolite fibre heated at 1000 °C showing the *d*-spacings in Å of the major diffraction lines. Legend: di = diopside; en = enstatite; cen = clinoenstatite.

Table 3. Final atomic coordinates, occupancies, and atomic displacement parameters (Å^2). * Fixed values from [31].

Site	ss	x/a	y/b	z/c	β_{11}	β_{22}	β_{33}	β_{12}	β_{13}	β_{23}	B_{eq}
tremolite RT											
M(4)	Ca	0	0.27763(4)	0.5	0.01141	0.01154	0.00881	0	0.00689	0	0.00981
M(1)	$Mg_{0.96}Fe_{0.04}$	0	0.08763(6)	0.5	0.00659	0.00786	0.00159	0	0.00197	0	0.00518
M(2)	$Mg_{0.92}Fe_{0.08}$	0	0.17701(6)	0	0.0056	0.0097	0.00412	0	0.00183	0	0.00636
M(3)	$Mg_{0.96}Fe_{0.04}$	0	0	0	0.00646	0.01077	0.00341	0	0.00116	0	0.0069
T(1)	Si	0.28028(7)	0.0841(4)	0.29657(1)	0.00479	0.00775	0.00248	0.00012	0.0012	0.00016	0.00496
T(2)	Si	0.2883(7)	0.17109(4)	0.80399(1)	0.00523	0.00834	0.00201	0.00009	0.00134	0.00099	0.00512
O(1)	O	0.111(1)	0.0862(1)	0.2175(2)	0.00667	0.00987	0.00183	0.00005	0.00168	0.00034	0.00602
O(2)	O	0.1188(2)	0.1712(1)	0.7243(3)	0.00755	0.01017	0.00307	0.00044	0.00285	0.00083	0.00666
O(3)	O	0.1113(2)	0	0.7181(3)	0.00832	0.00911	0.00363	0	0.00251	0	0.00684
O(4)	O	0.3644(2)	0.2476(1)	0.7912(3)	0.00947	0.00985	0.00691	0.00017	0.00319	0.00245	0.00854
O(5)	O	0.3462(2)	0.1337(1)	0.0988(3)	0.00713	0.01187	0.00474	0.00367	0.00128	0.00068	0.00795
O(6)	O	0.3435(2)	0.1185(1)	0.5889(3)	0.00601	0.0128	0.00484	0.00305	0.00175	0	0.00782
O(7)	O	0.3364(3)	0	0.2922(1)	0.0098	0.00926	0.00986	0	0.00285	0	0.00958
H *	H	0.206	0	0.771							0.03
tremolite 800 °C											
M(4)	Ca	0	0.27742(5)	0.5	0.01916	0.01465	0.01425	0	0.00871	0	0.01521
M(1)	$Mg_{0.96}Fe_{0.04}$	0	0.08723(6)	0.5	0.00758	0.00968	0.00366	0	0.00283	0	0.00672
M(2)	$Mg_{0.92}Fe_{0.08}$	0	0.17679(7)	0	0.01146	0.01112	0.00792	0	0.00303	0	0.01006
M(3)	$Mg_{0.96}Fe_{0.04}$	0	0	0	0.01448	0.00967	0.00675	0	0.00159	0	0.0105
T(1)	Si	0.28112(9)	0.08405(4)	0.29629(1)	0.01099	0.00973	0.00652	0.00027	0.00237	0.00022	0.00905
T(2)	Si	0.28851(9)	0.17096(4)	0.80355(2)	0.01159	0.0102	0.00668	0.00014	0.00257	0.00086	0.00944
O(1)	O	0.1121(2)	0.0860(1)	0.218(3)	0.01285	0.0115	0.00884	0.00028	0.00376	0.00003	0.01088
O(2)	O	0.1187(2)	0.1707(1)	0.7236(4)	0.01348	0.01295	0.00888	0.00067	0.00385	0.00085	0.01158
O(3)	O	0.1132(3)	0	0.7213(4)	0.01888	0.01288	0.01211	0	0.00542	0	0.01435
O(4)	O	0.3635(2)	0.2479(1)	0.7904(4)	0.01596	0.01214	0.01132	0.00102	0.00414	0.00227	0.01302
O(5)	O	0.3468(2)	0.1339(1)	0.0985(4)	0.013	0.01615	0.00913	0.00307	0.00313	0.00031	0.0127
O(6)	O	0.3444(2)	0.1188(1)	0.5877(3)	0.01307	0.01475	0.00883	0.00251	0.00285	0.00051	0.0122
O(7)	O	0.3373(3)	0	0.2925(5)	0.01578	0.01021	0.01607	0	0.00525	0	0.0138
H *	H	0.206	0	0.771							0.03

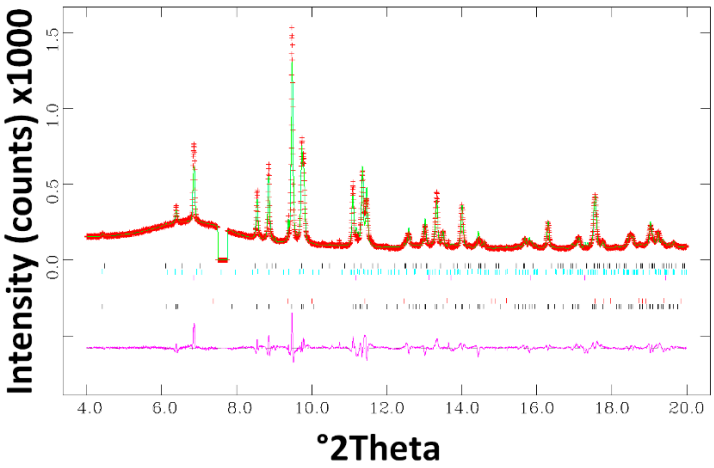

Figure 2. Graphical output of the Rietveld refinement of the bulk fibrous tremolite sample heated at 1000 °C. Legend: Red crosses = observed pattern; green line = calculated pattern; magenta line = difference curve. The markers plotted on five distinct rows correspond to the reflections of each phase in the model. Each row corresponds to a phase with diopside, calcite, cristobalite, clinoenstatite, and protoenstatite from the bottom to the top.

3.3. FEG-SEM Imaging

Figure 3 shows a selection of high resolution SEM pictures of the tremolite fibres after heating at 800 °C. The fibres bundles are still very long but invariably break perpendicularly to the fibre length (a) witnessing a fragile mechanical behaviour of the fibre after the thermal treatment. No clear signs of recrystallization are observed.

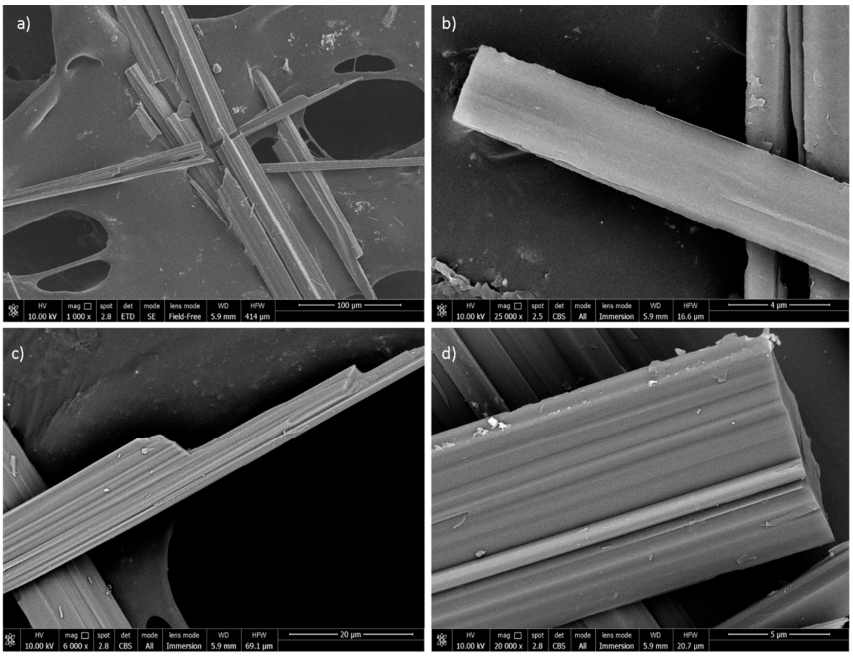

Figure 3. A gallery of field emission gun-Scanning electron microscopy (FEG-SEM) pictures of the tremolite fibres after heating at 800 °C. A group of very long fibre bundles (**a**); a single 3 µm thick fibres that broke with a perfect and sharp cleavage perpendicular to the fibre length (**b**); cleavage fragments of a former fibre bundle (**c**); high resolution image of a thick fibre bundle showing the single fibrils that broke perpendicular to the fibre length (**d**).

Figure 4 shows instead high-resolution SEM pictures of the tremolite fibres after heating at 1000 °C. Even the fibre bundles treated at 1000 °C are very long and regularly break perpendicularly to the fibre length, witnessing a fragile mechanical behaviour after the thermal treatment. No clear signs of recrystallization are observed for this sample, although the surface of the single fibres/fibrils display a rougher granular aspect, a marker of crystallization.

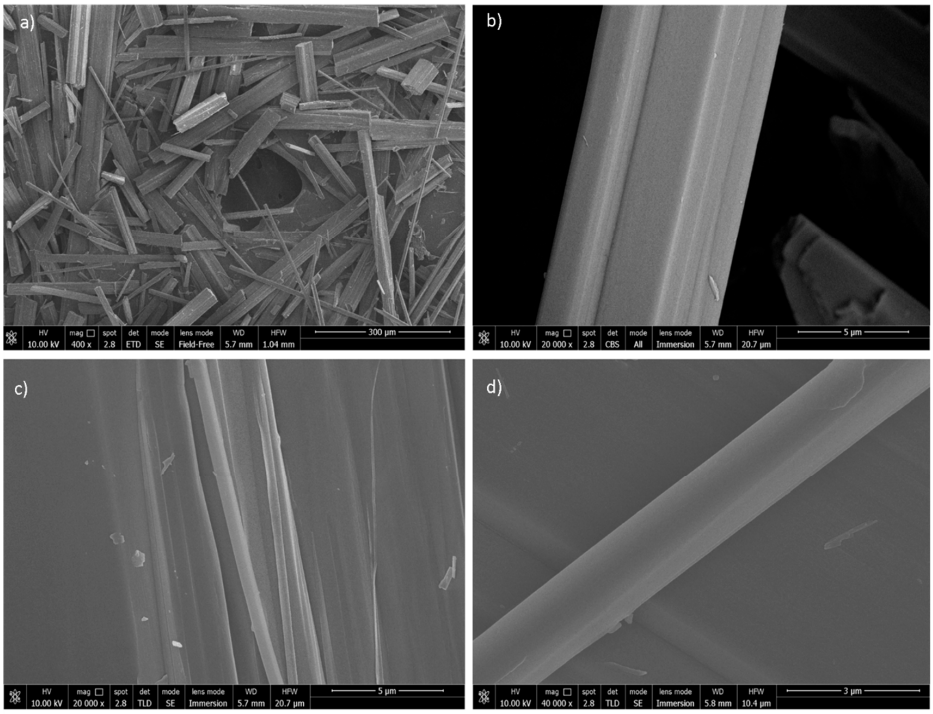

Figure 4. A gallery of FEG-SEM pictures of the tremolite fibres after heating at 1000 °C. Very long fibre bundles are shown together with elongated particles and cleavage fragments (**a**); no sign of surface recrystallization are clearly observed for the longer and thicker fibres (e.g., a single 5 µm thick fibre bundle shown on **b**) while single thin fibrils show more irregular and granular surfaces, possibly indicating recrystallization (**c**,**d**).

4. Discussion

4.1. Single Crystal Nano-Diffraction

The following structural data have been calculated using nano-focused synchrotron diffraction. The limited scattering power of the micrometer-sized crystals, the nature of the fibre bundles, and texture effects have been a limiting issue to collect and run structure refinements on such systems, so far. Diffraction data of nano-sized single crystals can be, indeed, now acquired with a beam size resolution that is currently similar to optical microscopes (hundreds of nm) using synchrotron radiation, as recently developed Si compound lenses allow unprecedented brilliance by nano-focusing [24,32].

As expected from the current knowledge of amphiboles crystal chemistry [14], at RT, the tremolite amphibole is monoclinic *C*2/*m* (Figure 5). The cell parameters are reported in Table 1 and are in agreement with the values found by Pacella et al. [31]. Mean tetrahedral bond lengths are reported in Table 4. The *T*(1)-O and *T*(2)-O tetrahedral bond lengths are slightly different to each other. The *T*(1)-O distances range from 1.604 Å to 1.635 Å, with an average value of 1.623, smaller than the *T*(2)-O ones, being, on average, 1.633 Å long. It is worthy of note that these values match the ones found for no tetrahedrally-coordinated Al in the structure [33]. Polyhedron distortion values, Δ, have comparable values for both *T*(1) and *T*(2) tetrahedra (Δ = 0.034 and Δ = 0.07, respectively, for *T*1 and *T*2), in line with [31].

The fractional site occupancy of the octahedral sites has been constrained to the values reported in Table 3. Examination of individual M-O bond lengths suggest that the average bond lengths for the *M*(1), *M*(2), and *M*(3) octahedra correlate well with mean ionic radius. In the octahedrally coordinated sites with *M*(2) > *M*(1) > *M*(3), for equivalent site occupancies, the mean bond length of the *M*(3) octahedron is approximately 0.015 Å smaller than those of the *M*(1) and *M*(2) octahedra. The *M*(1) and *M*(3) octahedra are slightly more regular than *M*(2), in terms of polyhedron distortion (Δ = 0.31 and Δ = 0.17). The *M*(4)-O length values for tremolite (2.497 Å) are typical of calcic amphiboles with *M*(4) sites fully occupied by Ca.

At high temperature, *a* is the unit cell axis that exhibits the largest expansion, while *c* the smallest, consistent with previous result obtained by Sueno et al. [22]. The β angle decreases getting closer to the value of β for pyroxenes [33]. The T sites exhibit very modest sensitivity to heat, as they undergo very slight changes with increasing temperature. The mean *T*(1)-(O) distances show almost no change and the *T*(2)-O distance increase, on average, by 0.002 Å. This can be explained as a result of the greater strength of the Si-O bonds relative to the *M*-O bonds. The *M*(1), *M*(2), *M*(3), and *M*(4) polyhedra show larger thermal expansions (Table 4) than do the silicate tetrahedra. The variations of individual *M*-O bonds at high temperature are shown in Table 3. Within the octahedral strip, the *M*(2) site shows the greatest angular deviation from a perfect octahedron, and the *M*(1) and *M*(3) sites show smaller and approximately similar deviations. This can be justified by its near position to the edge of the octahedral strip in the amphibole structure. The *M*(4) cation exhibits the smallest thermal expansion compared to the others M-O bonds present in the tremolite amphibole.

Table 4. Selected bond distances (in Å) for tremolite RT and 800 °C. Polyhedron distortion, Δ, as defined by [34], $\Delta = (1/n)\Sigma[(R_i - R)/R]^2$, where n is the number of ligands, R the average bond length, and R_i an individual bond length.

		RT	**800 °C**			**RT**	**800 °C**
T(1)	-O1	1.604592)	1.6124(2)	*T*(2)	-O2	1.6147(2)	1.6201(2)
T(1)	-O5	1.6325(1)	1.6377(2)	*T*(2)	-O4	1.5839(2)	1.5895(1)
T(1)	-O6	1.6357(2)	1.6391(2)	*T*(2)	-O5	1.6605(2)	1.6644(2)
T(1)	-O7	1.6202(2)	1.6236(1)	*T*(2)	-O6	1.674(2)	1.6807(2)
	average	1.623225	1.6282		average	1.633275	1.63867
	Δ	0.03483	0.079895		Δ	6.217863	6.577533
M(1)	-O1 ×2	2.0693(2)	2.0707(2)	*M*(2)	-O1 ×2	2.1418(2)	2.1499(2)
M(1)	-O2 ×2	2.0874(3)	2.1063(2)	*M*(2)	-O2 ×2	2.0908(2)	2.0974(2)
M(1)	-O3 ×3	2.0977(2)	2.0946(1)	*M*(2)	-O4 ×2	2.0265(2)	2.0374(2)
	average	2.0848	2.090533		average	2.086367	2.0949
	Δ	0.31706	0.50224		Δ	5.112674	4.813601
M(3)	-O1 ×4	2.0798(3)	2.0862(3)	*M*(4)	-O2 ×2	2.4024(2)	2.4116(3)
M(3)	-O3 ×2	2.0623(2)	2.0658(2)	*M*(4)	-O4 ×2	2.3248(3)	2.3334(2)
				M(4)	-O5 ×2	2.779(2)	2.7863(3)
				M(4)	-O6 ×2	2.5466(3)	2.5438(2)
	average	2.07105	2.076		average	2.5132	2.518775
	Δ	0.178499	0.241405		Δ	44.88401	44.25401

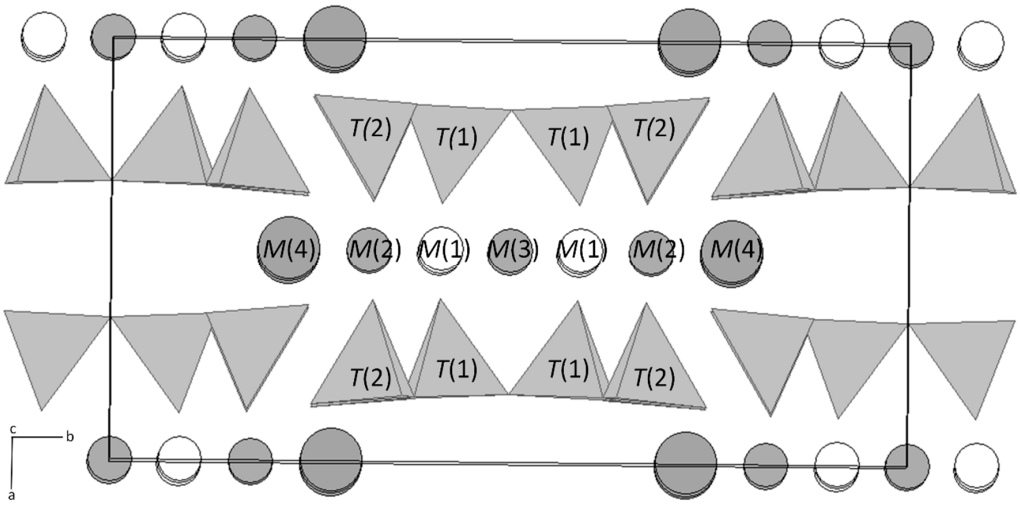

Figure 5. General view of the tremolite structure at room temperature (RT).

4.2. Tremolite Asbestos Fibres Heated at 1000 °C

The mineral assemblage observed at 1000 °C from the powder diffraction data confirms the results reported in the literature, with a recrystallization product basically composed of pyroxene phases and cristobalite [20]. Cristobalite apparently is not observed in the nano-diffraction data of the single fibre but is present in the bulk product, indicating that the kinetics of crystallization varies from fibre to fibre in a heterogeneous way, likely depending on the fibre size and surface area, with the bulk product that obviously represents a weighed overall contribution from all the single fibres.

The high resolution FEG-SEM images of the tremolite fibres after heating at 800 and 1000 °C all break perpendicularly to the fibre length, indicating a brittle mechanical behaviour after the thermal treatment. No clear signs of recrystallization morphology and pseudo-morphosis are observed, even for the fibres treated at 1000 °C that apparently underwent a crystal chemical reorganization with the nucleation of newly formed phase (see above). In fact, the microscopic analysis did not reveal any microstructure like the one observed for chrysotile treated at 1200 °C, with the fibres composed of an intergrowth of crystals of the newly formed silicates [11,35]. Minor signs of recrystallization, in the form of rough granular surfaces of the thinner fibres, evidence that the early pseudomorphic nucleation has not evolved yet into an extensive crystallization.

5. Conclusions

In this work, synchrotron nano-diffraction was applied for the first time to single fibres of asbestos tremolite and their high temperature reaction products at 800 and 1000 °C. Although the limited availability of synchrotron beams may restrict the procedure described in this paper to selected cases, using nano-sized beam may become a reliable routine for the structural characterization of fibre bundles. In fact, the high flux allows faster single crystal data collection of single nano-sized fibres, with higher signal-to-noise ratios. With this work, we have shown how this method is a powerful tool for the analysis of single fibres, even within fibre bundles, when powder X-ray diffraction or conventional single-crystal measurements fail.

On the basis of results of the structure refinements of the fibres at room temperature and at 800 °C, it is possible to say that:

1. The mean *T*-(O) distances have no sensitivity to heat, as they undergo a very slight expansion;
2. The *M*(1), *M*(2), *M*(3), and *M*(4) polyhedra exhibit larger thermal expansions than do the silicate tetrahedra, as a result of the weaker *M*-O bonds.

The fibres at 1000 °C underwent recrystallization and the Rietveld refinement performed on the sample heated at 1000 °C confirmed that the tremolite is fully transformed in a product basically composed of pyroxene phases and cristobalite.

The accompanying high resolution FEG-SEM study revealed that the tremolite fibres treated at 800 and 1000 °C all break perpendicularly to the fibre length, indicating a brittle mechanical behaviour after the firing process, although no clear signs of recrystallization and pseudo-morphosis are observed, even for the fibres treated at 1000 °C.

Author Contributions: A.F.G. conceived the research, took part to the nano-diffraction experiments and wrote the manuscript; C.G. and A.F.G. analysed the results and wrote the manuscript. D.D.G. and A.Z. performed the SEM analyses and discussed the results. M.Z. supported the SEM data collection. J.P.W. helped with the analysis of the diffraction data and discussed the results.

Acknowledgments: The authors thank the ESRF for provision of synchrotron beamtime. C.G. thanks Andy Fitch (ESRF) for the High Resolution Powder Diffraction data collected on ID22, Vadim Diadkin and Iurii Dovgaliuk for the useful discussions on single crystal refinements. This research was conducted within the granted Italian National PROGETTO DI UNA UNITA' DI RICERCA (PRIN) 2010–2011—prot. 2010MKHT9B 004 "Interazione fra minerali e biosfera: conseguenze per l'ambiente e la salute umana".

Conflicts of Interest: The authors declare no conflict of interest.

References

1. World Health Organization (WHO). *Asbestos and Other Natural Mineral Fibres: Environmental Health Criteria 53*; World Health Organization: Geneva, Switzerland, 1986; pp. 1–194. ISBN 92-4-154193-8.
2. European Community (EU) Parliament. Directive 2003/18/EC of the Council of 27th March 2003 amending Council Directive 83/477/EEC on the protection of workers from the risks related to exposure to asbestos at work. *Off. J. Eur. Union* **2003**, *97*, 48–52.
3. Gualtieri, A.F. Mineral fibre-based building materials and their health hazards. In *Toxicity of Building Materials*; Pacheco-Torgal, F., Jalali, S., Fucic, A., Eds.; Woodhead Publishing: Cambridge, UK, 2012; pp. 166–195. ISBN 978-0-85709-122-2.
4. Gualtieri, A.F. Introduction. In *Mineral Fibres: Crystal Chemistry, Chemical-Physical Properties, Biological Interaction and Toxicity*; Gualtieri, A.F., Ed.; European Mineralogical Union: London, UK, 2017; Volume 18, pp. 1–15. ISBN 0-903-05665-6.
5. International Agency for Research on Cancer (IARC). *Overall Evaluations of Carcinogenicity: An Updating of IARC Monographs Volumes 1 to 42*; International Agency for Research on Cancer: Lyon, France, 1987; pp. 1–440. ISBN 92-8-32-1411-0.
6. Gualtieri, A.F.; Giacobbe, C.; Sardisco, L.; Saraceno, M.; Gualtieri, M.L.; Lusvardi, G.; Cavenati, C.; Zanatto, I. Recycling of the product of thermal inertization of cement–asbestos for various industrial applications. *Waste Manag.* **2011**, *31*, 91–100. [CrossRef] [PubMed]
7. Gualtieri, A.F.; Boccaletti, M. Recycling of the product of thermal inertization of cement-asbestos for the production of concrete. *Constr. Build. Mater.* **2011**, *25*, 3561–3569. [CrossRef]
8. Kusiorowski, R.; Zaremba, T.; Piotrowski, J.; Podwórny, J. Utilisation of cement-asbestos wastes by thermal treatment and the potential possibility use of obtained product for the clinker bricks manufacture. *J. Mater. Sci.* **2015**, *50*, 6757–6767. [CrossRef]
9. European Commission (EC). Directive 2008/98/EC of the European Parliament and of the Council of 19 November 2008 on waste. *Off. J. Eur. Union* **2008**, *312*, 22.
10. Leonelli, C.; Veronesi, P.; Boccaccini, D.N.; Rivasi, M.R.; Barbieri, L.; Andreola, F.; Lancellotti, I.; Rabitti, D.; Pellacani, G.C. Microwave thermal inertisation of asbestos containing waste and its recycling in traditional ceramics. *J. Hazard. Mater.* **2006**, *135*, 149–155. [CrossRef] [PubMed]
11. Gualtieri, A.F.; Cavenati, C.; Zanatto, I.; Meloni, M.; Elmi, G.; Gualtieri, M.L. The transformation sequence of cement-asbestos slates up to 1200 °C and safe recycling of the reaction product in stoneware tile mixtures. *J. Hazard. Mater.* **2008**, *152*, 563–570. [CrossRef] [PubMed]
12. Dellisanti, F.; Rossi, P.L.; Valdrè, G. Remediation of asbestos containing materials by Joule heating vitrification performed in a pre-pilot apparatus. *Int. J. Miner. Process.* **2009**, *91*, 61–67. [CrossRef]

13. Bloise, A.; Catalano, M.; Gualtieri, A.F. Effect of Grinding on Chrysotile, Amosite and Crocidolite and Implications for Thermal Treatment. *Minerals* **2018**, *8*, 135. [CrossRef]
14. Hawthorne, F.C.; Oberti, R. Amphiboles: Crystal Chemistry. *Rev. Mineral. Geochem.* **2007**, *67*, 1–54. [CrossRef]
15. Dichicco, M.C.; Laurita, S.; Sinisi, R.; Battiloro, R.; Rizzo, G. Environmental and Health: The Importance of Tremolite Occurence in the Pollino Geopark (Southern Italy). *Geosciences* **2018**, *8*, 98. [CrossRef]
16. Bloise, A.; Kusiorowski, R.; Gualtieri, A.F. The Effect of Grinding on Tremolite Asbestos and Anthophyllite Asbestos. *Minerals* **2018**, *8*, 274. [CrossRef]
17. Bloise, A.; Kusiorowski, R.; Gualtieri, M.L.; Gualtieri, A.F. Thermal behaviour of mineral fibres. In *Mineral Fibres: Crystal Chemistry, Chemical-Physical Properties, Biological Interaction and Toxicity*; Gualtieri, A.F., Ed.; European Mineralogical Union: London, UK, 2017; Volume 18, pp. 215–252. ISBN 0-903-05665-6.
18. Wittels, M. Structural disintegration of some amphiboles. *Am. Mineral.* **1952**, *52*, 28–36.
19. Kusiorowski, R.; Zaremba, T.; Piotrowski, J.; Adamek, J. Thermal decomposition of different types of asbestos. *J. Therm. Anal. Calorim.* **2012**, *109*, 693–704. [CrossRef]
20. Bloise, A.; Catalano, M.; Barrese, E.; Gualtieri, A.F.; Gandolfi, N.B.; Capella, S.; Belluso, E. TG/DSC study of the thermal behaviour of hazardous mineral fibres. *J. Therm. Anal. Calorim.* **2016**, *123*, 2225–2239. [CrossRef]
21. Johnson, N.M.; Fegley, B. Tremolite decomposition on Venus II. Products, kinetics, and mechanism. *Icarus* **2003**, *164*, 317–333. [CrossRef]
22. Sueno, S.; Cameron, M.; Papike, J.J.; Prewitt, C.T. The High Temperature Crystal Ghemistry of Tremolite. *Am. Mineral.* **1973**, *58*, 649–664.
23. Pollastri, S.; Gualtieri, A.F.; Gualtieri, M.L.; Hanuskova, M.; Cavallo, A.; Gaudino, G. The zeta potential of mineral fibers. *J. Hazard. Mater.* **2014**, *276*, 469–479. [CrossRef] [PubMed]
24. Snigirev, A.; Kohn, V.; Snigireva, I.; Lengeler, B. A compound refractive lens for focusing high-energy X-rays. *Nature* **1996**, *384*, 49–51. [CrossRef]
25. Labiche, J.C.; Mathon, O.; Pascarelli, S.; Newton, M.A.; Guilera Ferre, G.; Curfs, C.; Vaughan, G.; Homs, A. The fast readout low noise camera as a versatile x-ray detector for time resolved dispersive extended x-ray absorption fine structure and diffraction studies of dynamic problems in materials science, chemistry, and catalysis. *Rev. Sci. Instrum.* **2007**, *78*, 09130. [CrossRef] [PubMed]
26. Rigaku Oxford Diffraction Ltd. *CrysAlis PRO*; Rigaku Oxford Diffraction Ltd.: Yarnton, UK, 2015.
27. Sheldrick, G.M. *SHELX97—Program Suite for the Solution and Refinement of Crystal Structures (Release 97-2)*; University of Göttingen: Göttingen, Germany, 1998.
28. Larson, A.C.; Von Dreele, R.B. *Generalized Structure Analysis System (GSAS)*; Los Alamos National Lab: Los Alamos, NM, USA, 1994.
29. Toby, B.H. EXPGUI, a graphical user interface for GSAS. *J. App. Cryst.* **2001**, *34*, 210–213. [CrossRef]
30. Pollastri, S.; D'Acapito, F.; Trapanati, A.; Colantoni, I.; Andreozzi, G.B.; Gualtieri, A.F. The chemical environment of iron in mineral fibres. A combined X-ray absorption and Mössbauer spectroscopic study. *J. Hazard. Mater.* **2015**, *298*, 282–293.
31. Pacella, A.; Andreozzi, G.B.; Ballirano, P.; Gianfagna, A. Crystal chemical and structural characterization of fibrous tremolite from Ala di Stura (Lanzo Valley, Italy). *Period. Mineral.* **2008**, *77*, 51–62.
32. Fahrnbauer, F.; Rosenthal, T.; Schmutzler, T.; Wagner, G.; Vaughan, G.B.M.; Wright, J.P.; Oeckler, O. Discovery and Structure Determination of an Unusual Sulfide Telluride through an Effective Combination of TEM and Synchrotron Microdiffraction. *Angew. Chem.* **2015**, *54*, 10020–10023. [CrossRef] [PubMed]
33. Hawthorne, F.C. Crystal chemistry of the amphiboles. *Rev. Mineral. Geochem.* **1981**, *9A*, 1–102. [CrossRef]
34. Shannon, R.D. Revised effective ionic radii andsystematic studies of interatomic distances in halides and chalcogenides. *Acta Crystallogr.* **1976**, *A32*, 751–767. [CrossRef]
35. Giacobbe, C.; Gualtieri, A.F.; Quartieri, S.; Rinaudo, C.; Allegrina, M.; Andreozzi, G.B. Spectroscopic study of the product of thermal transformation of chrysotile-asbestos containing materials (ACM). *Eur. J. Mineral.* **2010**, *22*, 535–546. [CrossRef]